Control Theoretic Analysis of Gas-evolution Oscillators

Gowtham Venkatraman, Mythra Varun Balakuntala Srinivasa Murthy
Department of Mechanical Engineering, Indian Institute of Technology Madras, Chennai, 600 036, India
E-mail: {me11b023,me11b038}@smail.iitm.ac.in

Abstract: Models that describe the dynamics of chemical oscillators are often associated with a delayed feedback. In this paper, we focus on one such model proposed by Bar-Eli and Noyes to explain the mechanism of gas-evolution oscillators. First, a local stability analysis of the system is performed to obtain the necessary and sufficient condition for stability. It is identified that the loss of stability occurs through a Hopf bifurcation. A measure for the rate of convergence of the system to its steady state is found using the Lambert W function. Further, the orbital stability of the bifurcating periodic solutions and the type of Hopf bifurcation is analysed. Finally, we perform a robust stability analysis of the linearised system using Vinnicombe gap metric for parametric uncertainties. This control theoretic analysis attempts to improve the mathematical understanding of the behaviour of gas-evolution oscillators.

Key Words: Gas-evolution oscillators, Local stability, Rate of convergence, Hopf bifurcation, Vinnicombe metric.

1 INTRODUCTION

Oscillating systems can possess nontrivial dynamic behaviour, especially if the system is nonlinear or comprises delayed feedback. One such system is a gas-evolution oscillator, modelled by a non-linear delay-differential equation in [2]. This is the major motivation for our control theoretic study of the model.

Reports of oscillatory gas evolution were observed in [9] during decomposition of organic acids. These are examples of systems called gas-evolution oscillators. Gas-evolution oscillators are chemical systems that exhibit oscillatory behaviour usually resulting from a non-instantaneous feedback mechanism [2]. Some examples are the decomposition of benzene diazonium salts, hydrogen peroxide and ammonium nitrite. The dynamics of ammonium nitrite decomposition is studied in [8]. Their characteristics are well described by delayed feedback models.

The physical picture may be understood from the following simplified explanation. A gaseous product, once produced in homogeneous solution, forms bubbles and rises to the surface where it escapes. It is this mechanism that induces delayed, negative feedback that is key to the onset of the oscillations. This delay causes pulsed evolution of gas, and these oscillations are sustained by the continuous production of the gas in solution.

Previous work in this area in modelling such gas evolution oscillators using delay-differential equations is found in [2], [4], [8]. For the purpose of our analysis, we use the delay-differential equation (DDE) model for gas-evolution oscillators proposed by Bar-Eli and Noyes [2]. This area continues to generate interest, as seen in [6], a recent study on modelling coupled biological oscillators as chemical oscillators with delayed feedback.

The organization of our paper is as follows. In Section 2, we describe the gas-evolution oscillator model and relations for evolution of concentration and pressure. In Section 3, we derive the sufficient and necessary and sufficient conditions for local stability. A necessary condition for local stability is obtained from a frequency domain analysis. Stability charts are constructed using the conditions for local stability. Section 4 contains an analysis of the rate of convergence behaviour of the linearised system using the Lambert W function. Extrema for the rate of convergence, perturbing one of the system parameters with the other kept fixed is also obtained. In Section 5, we conduct a local Hopf bifurcation analysis. In Section 6, we perform a local robust stability analysis in the frequency domain using the Vinnicombe gap metric.

2 THE MODEL

Here we present the model for the gas concentration $C(t)$ proposed by Bar-Eli and Noyes [2]. Bubble formation by homogeneous nucleation only starts when the solution's supersaturation crosses a critical value, denoted by C_{sat}. The nuclear bubbles thus formed grow to a certain size before escaping to the surface. The diffusion of dissolved gases molecules into the growing bubbles depletes the surrounding solution of gas molecules. This withholds further nucleation for several seconds until critical supersaturation is reached. This is the source of the delay term.

We denote rate constant by k_{nu}, saturation concentration by C_{sat}, and a constant α, using the notation given in [2]. The model is thus given by:

$$\frac{dC(t)}{dt} = R_{ch} - k_{nu}(C(t) - C_{sat}) \exp\left(\frac{-\alpha}{(C_\tau - C_{sat})^2}\right), \quad (1)$$

where $C_\tau = C(t-\tau)$.

Experimental results have suggested that C_{sat} can be approximated as a constant in the time scale of experimental observation. Such an assumption will not be valid indefinitely in a closed container. Using the transformation $x = C - C_{sat}$, we get

$$\frac{dx(t)}{dt} = R_{ch} - k_{nu}x(t)\exp\left(\frac{-\alpha}{(x(t-\tau))^2}\right). \quad (2)$$

Here R_{ch} denotes the rate of the reaction. R_{ch} is found to change sufficiently slowly that we can treat it as constant for the timescale of observation of the dynamics [2]. However, R_{ch} in any closed system must ultimately decay to zero because the chemicals are consumed. Here we implicitly assume that the decay timescale of the zero order kinetics is much larger than the time scale of observation.

The variation of pressure is given by the equation

$$\frac{dP(t)}{dt} = k_2 x(t)\exp\left(\frac{-\alpha}{x^2(t-\tau)}\right) - k_{fl}(P(t)-P_0)\,, \quad (3)$$

where k_{fl} is the first-order rate constant for flow of gas from the space above the solution to the external atmosphere at pressure P_0 and second term is leak to atmosphere, depending on vessel characteristics. For a closed container, $k_{fl} = 0$. Equations (2) and (3) are non-dimensionalised using the following substitutions:

$$\begin{aligned} x' &= \frac{x}{\sqrt{\alpha}}\,, & t' &= \frac{R_{ch}t}{\sqrt{\alpha}}\,, \\ k' &= \frac{k_{nu}\sqrt{\alpha}}{R_{ch}}\,, & p' &= \frac{(P-P_0)k_{nu}}{k_2\sqrt{\alpha}}\,, \\ k_1' &= \frac{k_{fl}\sqrt{\alpha}}{R_{ch}}\,. \end{aligned}$$

Dropping the primes on these definition, we obtain

$$\begin{aligned} \frac{dx(t)}{dt} &= f(x(t), x(t-\tau)) \\ &= 1 - kx\exp\left(\frac{-1}{x^2(t-\tau)}\right), \quad (4) \\ \frac{dp(t)}{dt} &= kx\exp\left(\frac{-1}{x^2(t-\tau)}\right) - k_1 p\,, \quad (5) \end{aligned}$$

which are dimensionless equations equivalent to equations (2) and (3), respectively. Clearly, equations (4) and (5) are not coupled, and equation (5) is extraneous to our analysis.

For ease of measurement, experimental measurements in the past have been of the pressure p above the solution. We are hence interested in its dynamics. Equations (4) and (5) can be simplified to

$$\frac{d}{dt}\big(x + p\exp(k_{fl}t)\big) = 1\,.$$

Clearly, in the case of a closed container, k_{fl} is 0, [2], the quantity $p(t) + x(t)$ varies at a constant rate with time. For non-zero k_{fl}, when there is a leak, pressure is explicitly related to concentration.

$$p(t) = exp(-k_{fl}t)(t - x(t))\,.$$

3 LOCAL STABILITY ANALYSIS

In this section, we linearise equation (4) about its steady state, and extract conditions for its local stability in terms of the parameters. After establishing the sufficient and necessary conditions for local stability, we construct stability charts, and represent these conditions in terms of the parameters k and τ of the nonlinear model.

For x_{ss} to be a steady state concentration, it should satisfy the following equation,

$$x_{ss}\exp\left(\frac{-1}{x_{ss}^2}\right) = \frac{1}{k}\,. \quad (6)$$

The derivative of the left hand side of equation (6) with respect to x_{ss},

$$\exp\left(\frac{-1}{x_{ss}^2}\right)\left(1 + \frac{2}{x_{ss}^2}\right),$$

is positive for all x, hence the left hand side of equation (6) is monotonically increasing, which means that the equation can have at most one solution. Thus, for k greater than zero, the model has a unique steady state. Let $y(t)$ be the perturbation in x about the steady state, such that $y(t) = x(t) - x_{ss}$. For a local analysis, $y(t)$ is small. So, we can expand the non-linear function in equation (4), about the steady state, using Taylor's series. Taking only the linear terms, we obtain

$$\frac{dy(t)}{dt} = \left.\frac{\partial f}{\partial x(t)}\right|_{x_{ss}} y(t) + \left.\frac{\partial f}{\partial x(t-\tau)}\right|_{x_{ss}} y(t-\tau)\,.$$

This results in a linear delay-differential equation in $y(t)$,

$$\frac{dy(t)}{dt} = -by(t-\tau) - ay(t)\,, \quad (7)$$

$$\text{where} \quad a = \frac{1}{x_{ss}}, \qquad b = \frac{2}{x^3{}_{ss}} = 2a^3. \quad (8)$$

From equations (6) and (8) we get

$$a = \sqrt{\frac{\mathrm{W}_0(2k^2)}{2}}\,, \quad (9)$$

where W_0 is the principal branch of the Lambert W function [10].

3.1 Time Domain Analysis

For the linear model described by equation (7), consider solutions of the form

$$y(t) = ce^{\lambda t}\,. \quad (10)$$

Substitution of this solution into the linear model gives us the characteristic equation for the linear model,

$$\lambda + be^{-\lambda\tau} + a = 0\,. \quad (11)$$

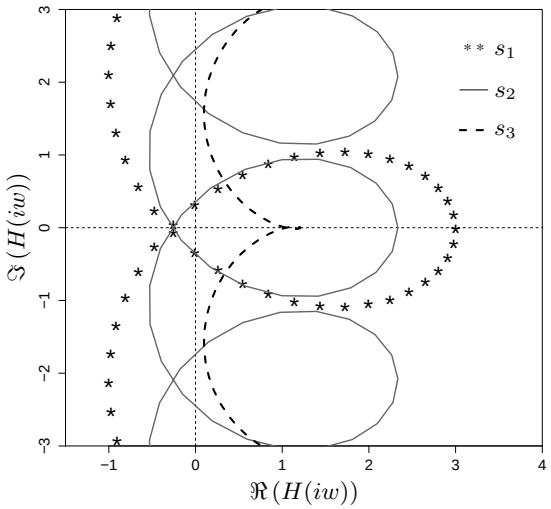

Figure 1: Nyquist plots at different states. Choice of system parameters in state s_1 is $k = e$, $\tau = 1.5$, for state s_2 is $k = 1$, $\tau = 2$ and those at state s_3 is $k = 2$, $\tau = 1$. $\Re$ denotes the real part and $\Im$ the imaginary part.

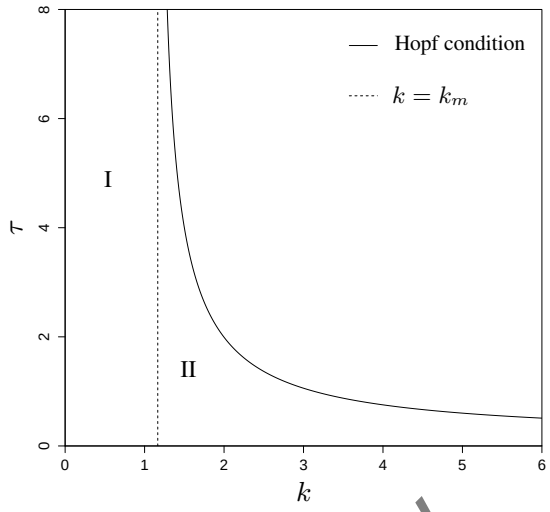

Figure 2: The solid curve represents the necessary and sufficient conditions for local stability the stability margin. The dotted line represents the sufficient condition given by the equation (20), where $k_m = 1.1658$. The region I represents the regime of non-oscillatory convergence and II the regime of oscillatory convergence.

The real part of solutions to equation (11) determine the stability of the linear model. Note that when $\tau = 0$, the equation will always have a real, negative solution, $\lambda = -(a+b)$, as $a,\ b > 0$. Therefore, in the absence of a time delay, the steady state x_{ss} will be stable in the local regime. We now substitute $\lambda = \mu + i\omega$ in equation (11), and equate the real and imaginary parts to zero to get

$$\begin{aligned} \mu &= -be^{-\mu\tau}\cos(\omega\tau) - a \\ \omega &= be^{-\mu\tau}\sin(\omega\tau)\ . \end{aligned} \tag{12}$$

Necessary and Sufficient Condition for Local Stability

For the steady state x_{ss} to be locally asymptotically stable, that is, for all trajectories $y(t)$ to converge to zero as $t \to \infty$, the real part of λ has to be negative. If $\mu < 0$, the steady state is stable. If $\mu > 0$, the steady state x_{ss} is unstable, and we know that the model exhibits sustained oscillations. Transition to instability occurs at $\mu = 0$, which gives us the margin of stability. At the stability margin ($\mu = 0$), denoting critical values of ω by ω_c and τ by τ_c, we have

$$\begin{aligned} \cos(\omega_c\tau_c) = -\frac{a}{b}\ ,\ \sin(\omega_c\tau_c) &= \frac{\omega_c}{b}\ , \\ \omega_c &= \sqrt{b^2 - a^2}\ , \\ \tau_c &= \left(\frac{1}{\sqrt{b^2-a^2}}\right)\cos^{-1}\left(-\frac{a}{b}\right)\ . \end{aligned} \tag{13}$$

For $b > a$, the steady state is locally stable if and only if the delay is less than the critical delay, i.e., $\tau < \tau_c$. For any value of k, the critical value of τ, is given by equation (13). Therefore, the necessary and sufficient condition for local stability of the steady state becomes

$$\tau < \left(\frac{1}{\sqrt{b^2-a^2}}\right)\cos^{-1}\left(-\frac{a}{b}\right)\ . \tag{14}$$

Sufficient Conditions for Local Stability

We now use the local stability analysis to obtain two sufficient conditions for stability. It is clear from equation (12) that the following inequality always holds true :

$$|\mu + a| \le |-be^{-\mu\tau}|\ . \tag{15}$$

We assume $b < a$. This implies

$$|b| < |a|\ . \tag{16}$$

Now we let $\mu > 0$. This implies

$$|\mu + a| > |a|\ , \text{ and} \tag{17}$$

$$|-be^{-\mu\tau}| < |b|\ . \tag{18}$$

Combining inequalities (16), (17) and (18), we find that

$$|\mu + a| > |-be^{-\mu\tau}|\ ,$$

which contradicts the result (15). Therefore the assumption $\mu > 0$ is wrong. So, if $b < a$, the condition $\mu < 0$ is always met, and the steady state is stable irrespective of the delay. A sufficient condition for local stability is thus

$$b < a\ . \tag{19}$$

Combining this with equation (8), we get $x_{ss}^2 \ge 2$. Substituting in equation (9) we obtain a condition on k,

$$k < \sqrt{\left(\frac{e}{2}\right)} = k_m\ , \tag{20}$$

which is a sufficient condition for local stability. Also note that if $b < a$, or $k < k_m$, from equation (12), no solutions to ω exist, and hence no oscillatory solutions to (7) exist.

Next we consider the case when $b > a$. Here, we take the necessary and sufficient condition obtained in (14).From here it is obvious that the condition

$$\tau < \min\left(\left(\frac{1}{\sqrt{b^2 - a^2}}\right)\cos^{-1}\left(-\frac{a}{b}\right)\right) = \frac{\pi}{2b}\,, \quad (21)$$

would be a sufficient condition for stability. This gives us the second sufficient condition for stability,

$$b\,\tau < \frac{\pi}{2}\,. \quad (22)$$

3.2 Frequency Domain Analysis

The above conditions for stability are demonstrated with the help of the Nyquist stability criterion. The Nyquist contour, which encircles the right half complex plane, is contructed and the corresponding Nyquist plot for the function,

$$H(s) = s + a + be^{-s\tau},$$

for different parametric values of k and τ are plotted in Figure 1. The Nyquist plot of $H(s)$, should not encircle the origin for the system to be stable. We observe that

$$\min(\Re(H(i\omega))) \;=\; a \;-\; b.$$

Thus, keeping the entire curve to the right of imaginary plane, $b < a$, is another sufficient condition for local stability, since the Nyquist plot will not encircle the origin once it is satisfied.

Thus, we have shown that the *sufficient conditions* for local stability are

$$\begin{aligned} a &\geq b\,, \text{ and} \\ b\tau &< \frac{\pi}{2}. \end{aligned}$$

3.3 Discussion of local stability conditions

Using the sufficient and necessary conditions for stability obtained in the previous section, we construct stability charts. Figure 2 depicts the margin of stability varying system parameters k and τ. Also note that $b = 2a^3$ from (8). This is a consequence of the fact that the nonlinear model being analysed has just one parameter besides the delay. This explicit functional dependence is now considered, and parameter b removed from the analysis, and only parameter k considered.

The stability chart in Figure 2 clearly gives us a picture of how the physical parameters of the gas-evolution oscillator affect its stability. The values of k and τ to the left of and below the curve, represent states in which the system decays to the steady state. In such systems, pulsed gas evolution may be observed at the start of the reaction, but the oscillations die down. The systems above the stability margin exhibit oscillatory gas evolution, that is sustained in a timescale small compared to the decay timescale.

Recall that the model parameter k is derived from the rates of nucleation and the rate of the reaction. Similarly, the delay τ is related to time taken for the bubble growth. This means that the stability of the system and the possibility of sustained oscillations in the product concentration are controlled by the relative rates of the two physical processes - nucleation and bubble growth.

4 CONVERGENCE ANALYSIS

In this section, we analyse how fast the linear model converges to the steady state, given that the necessary and sufficient condition for local stability is satisfied. This allows us to determine how quickly the pulsed gas evolution dies down in a stable system. We also identify regions of oscillatory and non-oscillatory convergence. The rate of convergence of $x(t)$ to the steady state value is assumed to be given by the magnitude of the real part of the root λ.

For $k < k_m$, $\omega = 0$, and hence from equation (12),

$$\mu = -be^{-\mu\tau} - a. \quad (23)$$

So for $k < k_m$, as a and b increase, the rate of convergence increases. When $k > k_m$, ω can have a non-zero value, and hence oscillations are possible. Figure 2 shows the stability margin, oscillatory and non-oscillatory convergence regimes. In figures 3 and 4, rate of convergence is plotted against k and τ.

A computational approach to analysing the rate of convergence, where the equation

$$(\lambda + a)\tau e^{(\lambda+a)\tau} = -b\tau e^{a\tau}\,,$$

is solved at several points in the region of stability, yields results which match those obtained analytically. Regions of oscillatory and non-oscillatory convergence are shown in Figure 3. As shown in Section 3, the model exhibits non-oscillatory convergence for $b < a$.

It is clear that as each system parameter monotonously increases with the other fixed, there is one value at which the rate of convergence peaks. Away from this value, the rate of convergence decreases monotonically. The physical interpretation of these would be as follows. For a fixed delay, by varying the rate of nucleation and reaction, oscillations, if present in the system, die down with a rate of convergence, which passes through a maxima.

For a system with parameters values near the margin of stability, pulsed gas evolution should be observed much longer, although the steady state is stable. Also note that the linearization has limited range of applicability of the model to a small region around the steady state. For systems with k less than k_m, oscillatory gas evolution is impossible.

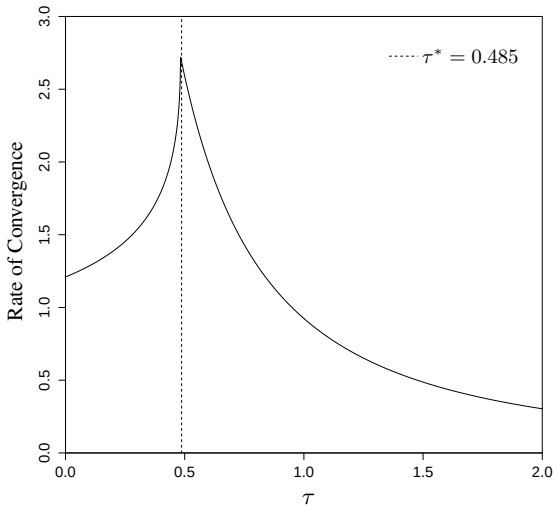

Figure 3: Variation of rate of convergence with parameter τ. Parameter k is fixed at 1. Maximum rate of convergence is achieved at $\tau = \tau^*$.

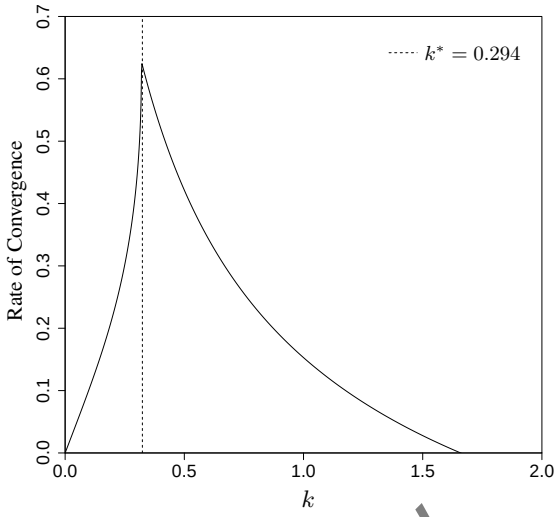

Figure 4: Variation of rate of convergence with parameter k choosing $\tau = 3$. Maximum rate of convergence is achieved at $k = k^*$.

4.1 Lambert W Analysis

Lambert W function is defined to be any function $W(H)$ that satisfies

$$W(H)\, e^{W(H)} = H.$$

It is complex valued, with a complex argument H, and an infinite number of branches, W_k, with k taking integral values. Solutions of equation (11) are given by [2].

$$\lambda_k = \frac{1}{\tau} W_k(-2a^3\tau \exp(a\tau)) - a,\ k\ \epsilon\ \mathcal{Z}.$$

This is an analytical expression directly relating the poles and the parameters of the equation, and hence stability analysis can be performed by finding the rightmost pole among all the poles. Although there are infinite poles, we know that the rightmost pole among them can be obtained from the principal branch (k = 0) as proved in [10], that is

$$\max(\Re(W_k(H))) = \Re(W_0(H)).$$

It is of considerable interest to identify for a given delay in a system, that choice of parameter k that can maximise the rate of convergence, depicted by k^* in Figure 4. From above equation derived using the Lambert W function, we now identify that there always exists one extrema of the rate of convergence, which coincides with the discontinuity of the real part of the primary branch of the Lambert W function. We identify that it occurs for $\Re(W_0(H))$, at $H = -1/e$. This condition is now used to maximise rate of convergence of the system to steady state by varying τ. τ^* denotes the value of τ, at a fixed k, for maximum rate of convergence.

$$\begin{aligned} a\tau^* \exp(a\tau^*) &= \frac{1}{2ea^2} \\ \tau^* &= \frac{1}{a} \mathrm{W}_0\left(\frac{1}{2ea^2}\right) \end{aligned}$$

Complementarily, we also identify, on fixing parameter k (and hence a, from equation (9)), the choice of delay that maximises rate of convergence of the system to steady state. Following a similar procedure, defining a^* similar to τ^*, we obtain,

$$a^* = \frac{3}{\tau} \mathrm{W}_0\left(\frac{1}{3}\left(\frac{\tau^2}{2e}\right)^{\frac{1}{3}}\right).$$

Bound on the rate of convergence with each system parameters fixed was computed. We obtain parameter values k^*, or τ^* maximising $\Re(\lambda_0)$ in each of the cases mentioned. Note that the global maxima of the rate of convergence, conditioned on one variable may not coincide with the said discontinuity, but the identified parameter value will correspond to a local maximum of rate of convergence.

5 LOCAL BIFURCATION ANALYSIS

In this section, a systematic local bifurcation analysis is carried out. First, we set out to prove that loss of local stability is through a Hopf bifurcation. Bifurcation plots are plotted with respect to system parameters k and τ.

We intend to study the system beyond the margin of local stability without perturbing the steady state. An exogenous non-dimensional parameter η is introduced as follows into the system in the following manner, motivated to drive the system just beyond the edge of local stability.

$$\frac{dx(t)}{dt} = \eta\left(1 - kx(t)\exp\left(\frac{-1}{(x(t-\tau))^2}\right)\right), \quad (24)$$

Here η is motivated to be a non-dimensional exogenous parameter which drives the above equation just beyond the locally stable regime. This leads to the linearised system

$$\frac{dx(t)}{dt} = \eta\left(ax(t) + b(x(t-\tau))\right).$$

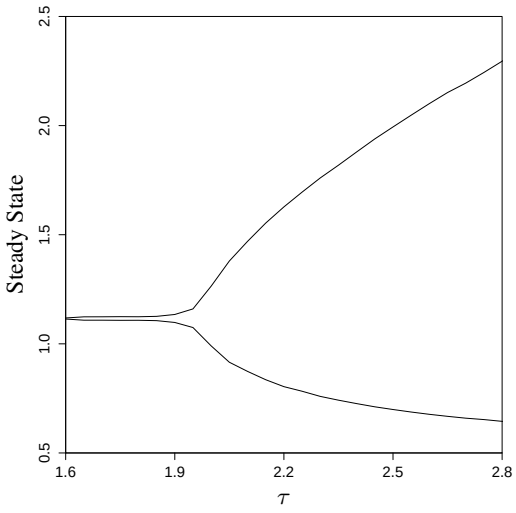

Figure 5: Bifurcation diagram for the system (4) for parameter τ. Fixing η at 1, using Hopf condition (25), fixing for the Hopf point $k_c = 2$, we observe a Hopf bifurcation at $\tau_c = 1.99$.

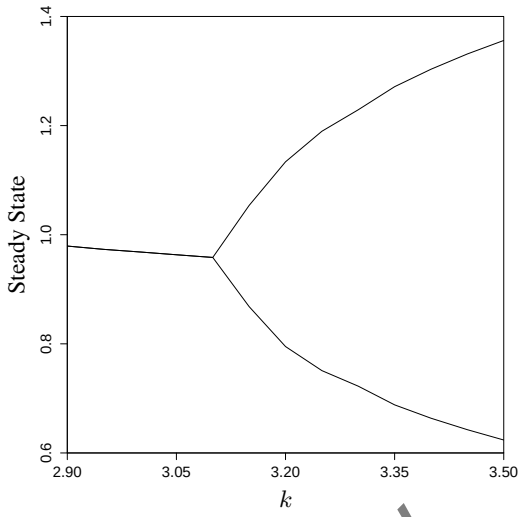

Figure 6: Bifurcation diagram for the system (4) for parameter k. Fixing η at 1, using Hopf condition (25), fixing for the Hopf point $\tau_c = 1$, we observe that a Hopf bifurcation occurs at k_c=3.134.

The characteristic equation is now

$$\lambda + \eta a + \eta b e^{-\lambda\tau} = 0.$$

We now proceed to verify the transversality conditions for the existence of a Hopf bifurcation for each of the system parameters and the exogenous parameter η. Note that the subscript c is used to denote the critical Hopf point.

$$\begin{aligned}
\Re\left(\frac{\partial\lambda}{\partial k}\right)\Big|_{k=k_c} &= \left(\frac{2a_c(a_c\tau_c+1)+3\omega_c^2\tau_c}{a_c\sqrt{(a_c\tau_c+1)^2+\omega_c^2\tau_c^2}}\right)a' \\
a' &= \frac{da}{dk}\Big|_{k=k_c} \\
\omega_c\tau_c &= \cos^{-1}\left(\frac{-1}{2a_c^2}\right) \\
\frac{da}{dk}\Big|_{k=k_c} &= \frac{1}{\exp(a_c^2)(1+2a_c^2)} > 0 \\
\Re\left(\frac{\partial\lambda}{\partial\tau}\right)\Big|_{\tau=\tau_c} &= \frac{-\omega_c^2}{a_c\sqrt{(1+a_c\tau_c^2)+\omega_c^2}} > 0 \\
\Re\left(\frac{\partial\lambda}{\partial\eta}\right)\Big|_{\eta=\eta_c} &= \frac{\omega_c^2\tau_c}{\eta_c\sqrt{(1+\eta_c a_c\tau_c)^2+\omega_c^2\tau_c^2}} > 0
\end{aligned}$$

Clearly, the transversality condition is satisfied for all parameters under consideration. Thus, we have now identified that the system undergoes a Hopf bifurcation at $\eta = \eta_c$, and at the Hopf condition, we choose η_c to be 1. The Hopf condition is given by the margin of local stability.

$$\left(\frac{1}{\sqrt{b_c^2-a_c^2}}\right)\cos^{-1}\left(-\frac{a_c}{b_c}\right) = \tau_c\eta_c\ , \qquad \text{where } a_c = \sqrt{\frac{\mathrm{W}_0(2k_c^2)}{2}}\ . \tag{25}$$

The characteristic equation of this system is given by

$$\lambda + \eta a + 2\eta a^3 e^{-\lambda\tau} = 0.$$

We now proceed to identify the type of Hopf bifurcation from the work of [7]. Then, we analyse the stability of the bifurcating periodic oscillations. Then, we utilize the analytical expressions, from [7], for the period and amplitude of the limit cycles formed by perturbation of η around eta_c. The system is perturbed about the critical Hopf point given by $\tau_c = 1.2092,\ k_c = \mathrm{e}$, where e is the base of the natural logarithm.

Note that the equation (4) is of the form:

$$\frac{d}{dt}x(t) = \kappa f\left(x(t), x(t-\tau)\right)$$

where the unique equilibrium of f is denoted by (x^*, y^*), where $y(t) = x(t-\tau)$. Define $u(t) = x(t) - x^*$, and take a truncated Taylor expansion of (4) including the linear, quadratic, and cubic terms to obtain

$$\begin{aligned}
\frac{d}{dt}u(t) &= \kappa\xi_x u(t) + \kappa\xi_y u(t-\tau) + \kappa\xi_{xx}u^2(t) \\
&+ \kappa\xi_{xy}u(t)u(t-\tau) + \kappa\xi_{yy}u^2(t-\tau) \\
&+ \kappa\xi_{xxx}u^3(t) + \kappa\xi_{xxy}u^2(t)u(t-\tau) \\
&+ \kappa\xi_{xyy}u(t)u^2(t-\tau) + \kappa\xi_{yyy}u^3(t-\tau) \\
&+ \mathcal{O}(u^4).
\end{aligned}$$

Now, let f^* denote evaluation of f at (x^*, y^*), the critical Hopf point.

$$\begin{aligned}
&\xi_x = f_x^*, && \xi_y = f_y^*, && \xi_{xx} = \tfrac{1}{2}f_{xx}^*, \\
&\xi_{xy} = f_{xy}^*, && \xi_{yy} = \tfrac{1}{2}f_{yy}^*, && \xi_{xxx} = \tfrac{1}{6}f_{xxx}^*, \\
&\xi_{xxy} = \tfrac{1}{2}f_{xxy}^*, && \xi_{xyy} = \tfrac{1}{2}f_{xyy}^*, && \xi_{yyy} = \tfrac{1}{6}f_{yyy}^*.
\end{aligned}$$

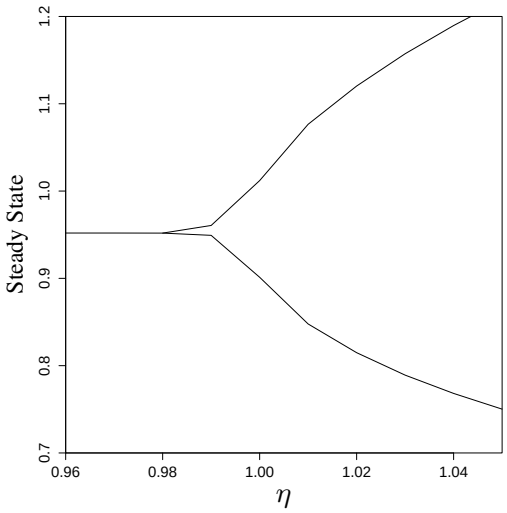

Figure 7: Bifurcation diagram for the system (4), fixing parameter values k at 3.135, and τ at 1. Using Hopf condition (25), we get $\eta_c = 1$.

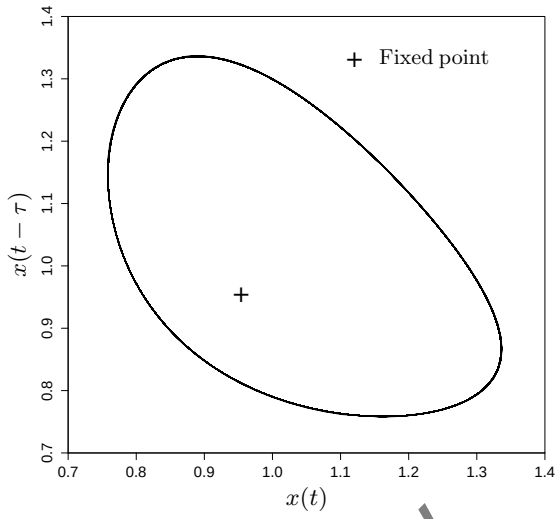

Figure 8: A stable limit cycle is formed at $\eta = 1.05$ at system parameters k and τ fixed at a Hopf point (given by $k = 3.135$ and $\tau = 1$). The steady state denoted by + is driven to instability, and a Hopf bifurcation has occurred.

The reader is referred to [5] and [7] for the theoretical basis and analytical characterization of the following analysis. The coefficients for the gas evolution oscillator, at sample values are found to be:

Term	Value	Term	Value	Term	Value
ξ_x	-1	ξ_y	-2	ξ_{xx}	0
ξ_{xy}	-2	ξ_{yy}	1	ξ_{xxx}	0
ξ_{xxy}	0	ξ_{xyy}	1	ξ_{yyy}	0.667

Now, we study the type and stability of the bifurcation and limit cycles formed with the exogenous parameter η. For illustration, the system is fixed at $k = \mathrm{e}$, and $\tau = 1.2092$. Computing requisite parameters, we find that $\mu_2 = 1.6135$. Thus, it is a *supercritical Hopf bifurcation*. We find that $\beta_2 = -2.6424$, the bifurcating periodic solution is *asymptotically orbitally stable*. Increasing the parameter η drives the system to instability, so choosing $\eta = \eta_c + \mu$ with $\mu = 0.05$, we find that:

Property		Values
Amplitude*	ϵ	0.05
Period	$\mathcal{P}$	3.6595
Floquet exponent	β	-0.0819

* Note that amplitude of the limit cycle is only of the order of ϵ.

Nomenclature of variables are the same as in the appendix of [7], and the reader is referred to the same for further information on the derivation. The numerical simulations were conducted using the scientific computing softwares MATLAB and XPP.

6 LOCAL ROBUSTNESS ANALYSIS

The conditions for local stability are dependent on system parameters k and τ. These parameter values may intrinsically have a degree of uncertainty, or could be susceptible to fluctuate in the course of the reaction, for example, due to temperature sensitivity. As the reaction proceeds, depending on the reaction enthalpy, temperature is susceptible to change, giving rise to perturbations in system parameters. We see the need to set bounds on these parametric uncertainties as these changes could drive the system to instability. This motivates us to perform a local robust stability analysis.

In this section, we analyse the robustness of the linear model of the system defined by (7), using the Vinnicombe or gap metric for bounded variations in the closed loop transfer function, using unit feedback, to define a bound on parameters for robust performance. We obtain the closed loop transfer function from the characteristic equation by equating it to $1 + P(s)$, thus obtaining the open loop transfer function $P(s)$. We observe

$$P(s) = \frac{b \exp(-s\tau)}{s + a}.$$

6.1 Vinnicombe Metric Technique

To define perturbations to the closed loop transfer function, we use the Vinnicombe or gap metric δ_v defined by Vinnicombe [11]. We use a bound on the gap metric to ensure robust performance of the feedback system, stated in [1]:

$$\delta_v(P_1, P_2) < 1/3\,. \tag{26}$$

Closed loop transfer function for the model is given by

$$G(s) = \frac{P(s)}{1 + P(s)}.$$

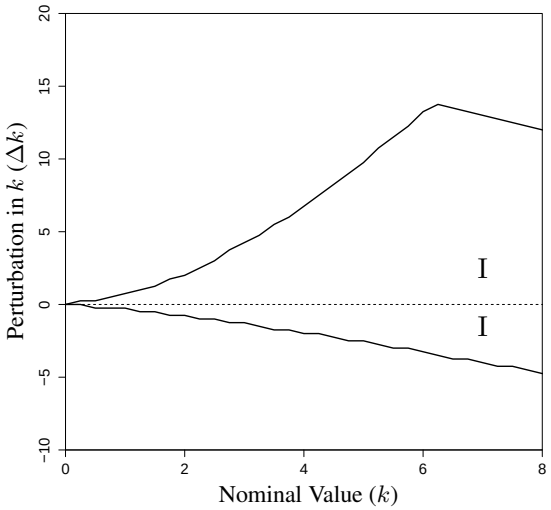

Figure 9: The bounded region marked as I denotes the bound for uncertainty(Δk) in parameter k on varying k, to ensure local robust stability, evaluated from the Vinnecombe metric condition (26). Parameter τ is fixed at 1.

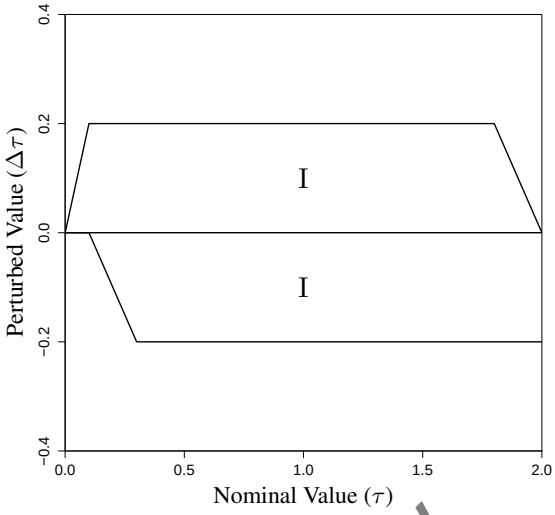

Figure 10: The bounded region marked as I denotes the bound for uncertainty($\Delta\tau$) in parameter τ on varying τ, to ensure local robust stability, evaluated from the Vinnecombe metric condition (26). Parameter k is fixed at e.

In the metric, we also note that the known system state is at P_1, and the uncertain model is denoted by P_2. For parametric uncertainty analysis of parameter k, delay is considered fixed, and parametric uncertainty is attached to the system parameter k. Similar analysis is repeated for τ.

Applying the condition (26), we obtain plots for allowed uncertainty in parameter values for robust performance. Using the given bound on δ_v, we obtain limits on perturbations about any system point, as illustrated in Figure 10. We thus obtain a band limiting the parametric uncertainties to guarantee robust performance of the closed loop system.

7 OUTLOOK

Our work aims to add to the present understanding of gas-evolution oscillators, improving the previous analysis performed by Bar-Eli and Noyes [2]. To this end, we performed a control theoretic study of the system, encompassing local stability, local bifurcation, rate of convergence, and local robustness analysis of the model. The rate of convergence of the linearised model to its steady state was studied, classifying regions of non-oscillatory, and oscillatory convergence, and its variation with parameters.

At an arbitrarily chosen system point, it was established that the model undergoes a supercritical Hopf bifurcation at the margin of local stability with an exogenous parameter η. Also, the resulting limit cycle is found to be asymptotically orbitally stable, using the approach in [7]. A local robust analysis was performed on the model, using the Vinnicombe or gap metric, defined in [11]. We hence obtained bounds on parametric variation for robust performance of the unit feedback system.

REFERENCES

[1] K. J. Åstrom and R. M. Murray, Feedback Systems: An Introduction for Scientists and Engineers, Princeton: Princeton University Press, Chap. 12, 2012.

[2] K. Bar-Eli and R. M. Noyes, Gas-evolution oscillators: A model based on delay equation, Journal of Physical Chemistry, Vol. 96, No.19, 7664-7670, 1992.

[3] T. Chevalier, A. Freund and J. Ross, The effects of a nonlinear delayed feedback on a chemical reaction, Journal of Physical Chemistry, Vol.95, No.1, 308-316, 1991.

[4] I. R. Epstein, Differential delay equations in chemical kinetics: Some simple linear model systems, Journal of Chemical Physics, Vol.92, No.3, 1702-1712, 1990.

[5] B. D. Hassard, N. D. Kazarinoff and Y. H. Wan, Theory and Applications of Hopf Bifurcation, Cambridge: Cambridge University Press, Chap. 1, 1981.

[6] V. Horvath, P. L. Gentili, V. K. Vanag and I. R. Epstein, PulseCoupled Chemical Oscillators with Time Delay, Angewandte Chemie International Edition, Vol.51, No.28, 6878-6881, 2012.

[7] G. Raina, Local bifurcation analysis of some dual congestion control algorithms, IEEE Trans. on Automatic Control, Vol.50, No.8, 1135-1146, 2005.

[8] M. B. Rubin, R. M. Noyes and K. W. Smith, Gas-evolution oscillators. 9. A study of the ammonium nitrite oscillator, Journal of Physical Chemistry, Vol.91, No.6, 1618-1622, 1987.

[9] K. W. Smith, R. M. Noyes and P. G. Bowers, Gas-evolution oscillators: Some new experimental examples, Journal of the American Chemical Society, Vol.105, No.9, 2572-2574, 1983.

[10] Sun Yi, P. W. Nelson and A. G. Ulsoy, Time Delay Systems: Analysis and Control using the Lambert W Function, Singapore: World Scientific, Chap. 5, 2010.

[11] G. Vinnicombe, Frequency domain uncertainty and graph topology, IEEE Trans. on Automatic Control, Vol.38, No.9, 1993.